AUTOMATIC CRATER MORPHOMETRY EXTRACTION. Sylvain Breton[1] and Cathy Quantin Nataf[1], [1]Université Lyon 1, France (sylvain.breton@ens-lyon.fr)

Introduction: Impact crater morphology analysis is a powerful tool to decrypt the evolution of planetary surfaces [1][2]. Indeed, the morphology of an impact crater evolves according to the resurfacing processes it undergoes. Erosion for instance, reduces the depth of a crater with time but the velocity of the process depends on the erosion style (eolian or fluvial for instance) [1]. The morphology of the impact craters is thus crucial parameters to characterize and quantify the erosion history of a planet. It is especially relevant for Mars where the climate history is complex.

One of the most used parameter in crater morphology is the ratio between the crater depth and its diameter. Assuming the initial depth of the crater, this parameter depends on the erosion rate but also on the age of the crater [3]. For impact craters smaller than a hundred meters, target properties may affect the initial crater/depth ratio [2]. In addition secondary craters are also supposed to be shallower than primaries [4].

However, to date, no large measurement set has allowed to address this issue regardless of the planetary surface. Indeed extracting those morphology parameters on individual craters is time-consuming as it requires accurate topographic data for each crater.

Here we propose a new automatic method providing large measurement set of depth/diameter ratio. We explain the method and its applications to the surface of Mars observed at high spatial resolution. As preliminary results we extract more than 3000 values of depth on different regions of Mars. We also discuss the limitations as well as the perspectives of this study.

Data and Methods: We use CTX (Context Camera) images from MRO (Mars Reconnaissance Orbiter) mission. After several year of mission, increasing coverage of the Mars surface by CTX images allows to create many digital elevation models (DEM) from two images taken on a different angle using stereo-photogrammetry. Those DEMs are associated with ortho-images that are aligned with the DEMs.

All the management of CTX images from images download and calibration to DEM and ortho-images calculation were done thanks to MarsSI facility [5][6]. MarsSI facility is using the AMES stereo-pipeline [7] to produce CTX DEMs and ortho-images on demand [5]. The calculated DEMs have the spatial resolution of the used CTX images (around 6 m/pixels). The resulted DEMs may have artifacts or bad pixels due to correlation issues. In order to remove these artifacts, we resample the DEMs at 20 m/pixels.

We perform impact crater mapping on the ortho-images under GIS environment (QGIS). Each crater is represented by a circle drawn from 2 points on the edge of the rim. We use a tool from GRASS software that extracts statistics from the associated DEM inside each crater circle. We extract for each crater the minimum, the maximum, the mean, the first and last deciles of both elevation and slope.

The depth of the crater is calculated as the difference between the elevation minimum and maximum or between the elevation first and last deciles. The use of the first and last deciles aims to eliminate extreme values introduced by local perturbations such as boulders or artifacts from the DEM computation. The potential bias in precision of this automatic measurement on individual crater is expected to be compensated by the large number of measurements.

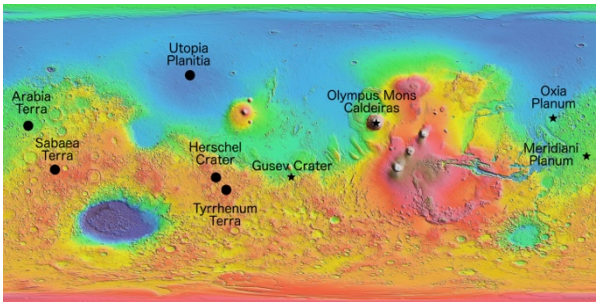

Figure 1: *Map of the investigated areas. We chose areas of interest (stars) and random sites (circles).*

We investigate several areas in different geological units, different latitudes and elevations in order to get a large set of data in different contexts (Figure 1). We analyze Gusev crater and Meridiani Planum where erosion has been investigated in situ [8]. We also investigate high elevation calderas where the atmospheric pressure is lower and the volcanic nature of the rock is constrained. We finally select several random areas in Noachian Highlands and in the north plains. The area studied in Sabaea Terra, displayed in blue in Figure 2, corresponds to the ejectas of a double-layered crater where auto-secondary crater production can be observed. The second area, displayed in Figure 2 in red, is located in Tyrrhenum Terra on a ridged plain.

Preliminary Results: As preliminary results we present here the data set obtained on the area in Sabaea Terra and the area in Tyrrhenum Terra. Figure 2 represents the evolution of depth according to the diameter of the craters. The diameters of the studied craters range from 20 m to 1 km. The associated depths vary from

filled craters (0 m) to 300 m. The relation between depth and diameter seems to follow a scaling law as shown by the logarithmic scale.

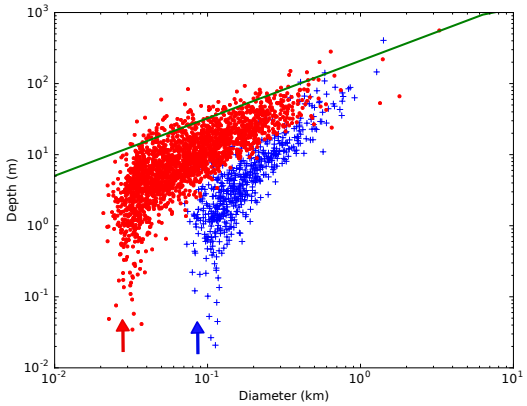

Figure 2: *Evolution of the crater depth as a function of their diameter. Depth is calculated as the difference between the extremum values of elevation The data set from Tyrrhenum Terra is represented as red dots and the data from Sabaea Terra is displayed in blue. The scaling law from Garvin and Frawley [9] for fresh craters is represented in green.*

As an indication, we compared our data with the scaling law of from Garvin and Frawley [9] (equation (1)) for depth of fresh craters on Mars.

$$\mathbf{(1)} \qquad \boldsymbol{d(D) = 0.21 * D^{0.81} \; if \; D < 7 \; km}$$

All our measures lie under this scaling law suggesting many craters have been modified. As the size of our data set will grow, we will be able to perform better comparison with this scaling law.

The two sites present a very different distribution of the depths. The crater depths of Sabaea Terra site range in lower depths than. Tyrrhenum Terra site. We propose here two hypotheses. This could be explained by a difference in the property of the impact target or by the occurrence of secondary craters in Sabaea Terra site that are supposed to be less deep than primaries [4]. Additional work will confirm either of the hypothesis.

In order to further exploit our data, we introduce the depth frequency distribution, by analogy with the size frequency distribution. The bins of depth are created as a percentage of the maximum depth. Figure 3 represents Tyrrhenum Terra data in the depth-diameter space. The data show a wide range of depths for a same diameter. We can see that the number of craters increases for shallower craters. Such depth distribution may be explained by the current erosion or infilling of small craters on Mars. This hypothesis needs further work to be confirmed.

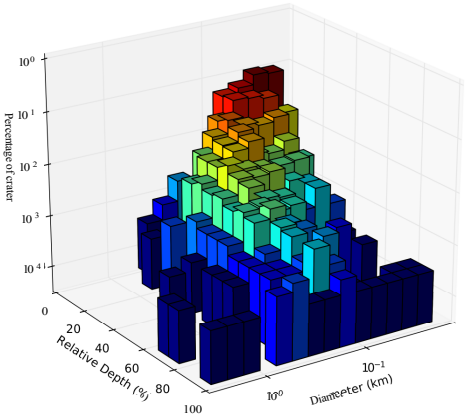

Figure 2: *Distribution of the craters in the diameter-depth space. The result is expressed as the percentage of craters in each bin relative to the total number of craters. The depth is expressed as a percentage of the maximum observed depth in a specific diameter bin.*

Future works: In the near future, we will calibrate our method comparing the depth found with our method with topographic profiles of a selection of craters. We will also collect data on additional regions to improve our data base of crater/depth ratios for craters smaller than 100 m. To do so we will perform new crater mapping on other areas of Mars trying to cover a wide range of ages and current climatic conditions (temperature, wind...). We will also investigate other diameter ranges down to CTX range by using HiRISE DEM and above CTX scale with HRSC and MOLA data.

Conclusion: We developed a new method to automatically extract statistics on crater morphometry. The method is powerful to extract large data set. The method applied on Mars, at multiple scales, will provide key clues on local erosion conditions or rock properties and, at large scale, on past sedimentary processes (erosion/infilling).

Acknowledgements: The research leading to these results has received funding from the European Research Council under the European Union's Seventh Framework Program (FP7/2007-2013)/ERC Grant agreement n° 280168. We thank M. P. Golombeck and N. Warne for the crater mapping they provided on Meridiani Planum.

References: [1] R.A. Craddock (1997) *JGR, 102,* 13321–13340. [2] D. Viola et al. (2017) *Icarus 284*. [3] NK. Forsberg-Taylor et al. (2004) *JGR, 109*. [4] R. J. Pike and D.E. Wilhelms (1978) *LPS IX*. [5] Quantin et al. (Submitted 2017) *PSS*. [6] Poulet et al. (Submitted 2017) *PSS*. [7] D.E. Shean et al. (2016) *JPRS, 116*. [8] M. P. Golombek et al (2006) *JGR, 111*. [9] J.B. Garvin and J.J. Frawley (1998) *GRL, 25,* 4405–4408.